Relative Importance of Mineralogy and Organic Matter Characteristics on Macroaggregate and Colloid Dynamics in Mg-Silicate Dominated Soils

Falsone G., Celi L., Stanchi S., Bonifacio E. Relative Importance of Mineralogy and Organic Matter Characteristics on Macroaggregate and Colloid Dynamics in Mg-Silicate Dominated Soils. LAND DEGRADATION & DEVELOPMENT. 27 (7) pp: 1700-1708.
DOI: 10.1002/ldr.2516

The publisher's version is available at:
http://doi.wiley.com/10.1002/ldr.2516

Title

RELATIVE IMPORTANCE OF MINERALOGY AND ORGANIC MATTER CHARACTERISTICS ON MACROAGGREGATE AND COLLOID DYNAMICS IN Mg-SILICATE DOMINATED SOILS

Short title

AGGREGATION IN Mg-SILICATE DOMINATED SOILS

Authors:

Gloria Falsone [a], Luisella Celi [b], Silvia Stanchi [b,c], Eleonora Bonifacio [b]

[a] DIPSA – Alma Mater Studiorum University of Bologna, via Fanin 40, 40127 Bologna, Italy

[b] DISAFA, University of Torino, Largo P. Braccini 2, 10095 Grugliasco (TO), Italy

[c] NATRISK, Research Centre on Natural Risks in Mountain and Hilly Environments, University of Torino, Largo P. Braccini 2, 10095 Grugliasco (TO), Italy

Corresponding author:

Eleonora Bonifacio: tel +39 011 670 8516, fax +39 011 6708692, E-mail Eleonora.Bonifacio@unito.it

ABSTRACT

Soil aggregation and organic matter conservation are important in the prevention of land degradation. Aggregation processes and organic matter turnover influence each other and depend on the characteristics of both minerals and organic pools. We assessed the relative importance of the organic and mineral phases at the macroaggregate and colloidal scale in two soils (CHL and SRP, chlorite and serpentine-rich, respectively) where Mg-silicates dominated, by incubating them with a relatively degraded and oxidized organic fraction, i.e. the humic acids (HA) extracted from the organic horizons of both CHL and SRP. The HA from SRP were more aromatic and richer in phenolic groups, whereas HA from CHL were N-richer, more aliphatic and richer in carboxyl groups. The SRP soil formed larger amounts of macroaggregates, more stable than in CHL. At the colloidal scale, SRP was more flocculated and clay had a lower electrophoretic mobility than CHL. HA enhanced aggregate formation in both samples but improved aggregate stability only in CHL. In CHL slight differences in electrophoretic mobility were visible, while in SRP differences were more pronounced, with a PZC at lower pH and larger hydrodynamic diameter. The abundance of Mg in SRP may have favoured the formation of weaker outer-sphere interactions and the release of clay-HA associations upon water dispersion, while in CHL Ca formed more stable bonds with HA. In SRP ligand exchange reactions can be ruled out, conversely to the dominant bonding mechanism occurring in Al-silicate dominated soils, with important consequences on the release of organic matter-loaded clay particles.

KEYWORDS: oxidized organic matter, aggregate stability, zeta potential, soil mineralogy, serpentine

INTRODUCTION

Soils are a finite resource sustaining terrestrial life and providing a wide set of ecosystem functions that are vital for the human kind, such as food and biomass production, carbon regulation, filtering pollutants, biodiversity and natural/cultural heritage (Adhikari & Hartemink, 2016; Berendse et al., 2015; Keesstra et al., 2012). However, soil degradation is an ongoing process often leading to permanent loss, putting at risk soil quality and availability for future generations. Land degradation is the result of a large number of natural and man-induced processes (Seeger & Ries, 2008; Zhang et al., 2015) that affect the topsoil chemical and physical quality and globally decrease soil functionality (Brevik et al., 2015). Among the main effects of land degradation, the breakdown of soil structure and disruption of aggregates are widely studied (De Clercq et al., 2015) as they are good indicators of poor soil quality (Zornoza et al., 2015). Soil structure and aggregate stability are directly impacted by land use (Cerdà, 2000; de Oliveira et al., 2015) and enhanced in natural and forest ecosystems or upon afforestation (Muñoz-Rojas et al., 2015) and tree plantation (Gümüs & Şeker, 2015). By affecting soil infiltration capacity, soil aggregates play a key role in controlling erosion processes and soil losses in semiarid areas and in areas that have lost their original vegetation cover (Arjmand Sajjadi & Mahmoodabadi, 2015; Cerdà, 1996; Mataix-Solera et al., 2011).

In addition to the well-known effect that soil structure and aggregates have on soil fertility, gas exchanges, and on the hydrological cycle, they significantly influence organic matter stocks and are thus fundamental in the carbon cycle (Six & Paustian, 2014; Chaplot & Cooper, 2015; O'Rourke et al., 2015). The inclusion of organic residues increases the stability of macroaggregates, although the highest residence time is recorded for clay-associated OM (Gelaw et al., 2013). A complex relationship between OM and aggregates therefore exists in soils: aggregation is favoured by OM, but in turn aggregates largely control the dynamics of organic pools (Six et al., 2004; Kögel-Knabner et al., 2008; Stanchi et al., 2015). Typically, OM in microaggregates is more stable and less sensitive to changes in land use (Debasish-Saha et al., 2014). Macroaggregates instead include also fresh residues that may undergo further transformation if aggregate turnover is slow enough to allow the physical protection of OM (Six et al., 2004). The addition of fresh, bio-labile organic compounds has a short term effect on soil aggregation processes, while treating the soil with more degraded and oxidized organic materials may lead to a stable improvement of soil physical characteristics (Piccolo & Mbagwu, 1999; Abiven et al., 2009; Mamedov et al., 2014; Mikutta et al., 2015). The effect of these molecules on soil aggregation depends, however, on the availability of reactive mineral surfaces and dispersion/flocculation behaviour of the colloidal fraction (Amezketa, 1999; Vogel et al., 2014). Denef et al. (2002) observed that soils with dominating variable charge clay minerals have a greater potential to form stable macroaggregates when OM concentrations are low, while the greatest response in stable macroaggregate formation with additional organic inputs was found in soils with mixed mineralogy, likely because of the occurrence of different binding mechanisms. Also the characteristics of organic material affect the mechanisms involved in the reactions with mineral surfaces by determining both bonding extent and strength (Mikutta et al., 2007). The presence of this large set of controlling variables makes the study of the effect of organic matter on aggregation challenging, and field studies are mostly limited to the description of statistical correlations (Regelink et al., 2015). Laboratory

experiments of aggregate building up may be more suitable for understanding the relative role of several controlling variables without having to deal with excessive complexity, and therefore widely used to evaluate the effect of different pools of organic matter on aggregation (Ding et al., 2013; Andruschkewitsch et al., 2014; Vogel et al., 2014). However, most studies were carried out on kaolinites, smectites and vermiculites, or on soils where these Al-silicates dominated. Magnesium-rich phyllosilicates, such as serpentines (1:1) and lithogenic chlorites (2:1:1), are less frequent, but are often found in alpine regions and on peri-Alpine floodplains (Legros, 1992). Due to the different chemical properties of Al and Mg, the extent of direct bonding of OM to phyllosilicate surfaces should sharply differ and the results obtained with Al-silicates might not be directly applied to chlorite- or serpentine-dominated soils.

From previous studies, we found that the aggregation process induced by water-only wet and dry cycles differed in serpentinic and chloritic soils; clay-sand interactions prevailed in aggregate building up when the clay fraction was dominated by serpentine, while interactions between clay particles prevailed in the chloritic soil (Falsone et al., 2007). In this study, we hypothesized that the input of degraded, oxidized organic substances during wet and dry cycles might promote particle aggregation depending on their characteristics and soil mineralogy. The aim of this work was therefore to evaluate the relative importance of soil mineralogy and of the characteristics of added OM on aggregation and aggregate stability, both at the macroaggregate and colloidal size-scale. We also evaluated the differences in aggregate properties caused by the addition of organic matter by comparing the results with those obtained in the previous wet and dry experiment.

MATERIALS AND METHODS

The study area

The study area was located in north-western Italy (45°10'N, 7°23'E; Col del Lys). Two soils were selected in the area belonging to the greenstone belt of the Alps, a complex mix of ophiolites with micaceous, chloritic and calcareous schists. In the study area the soil parent material differs therefore in mineral abundance. One selected soil developed from chlorite-schists (CHL), and the other one was on serpentinite (SRP). They were described and classified as Typic Udorthent and Typic Hapludalf, respectively (Soil Survey Staff, 2014). The dominant vegetation consisted of grassland, although some larch trees were present at SRP. Soil samples were collected from the second horizon (AC and A2, respectively) after discarding the first A horizon to reduce the effect of native organic matter. The amount of organic carbon was less than 30 g kg^{-1} and quite similar between the two soil samples; the soils differed for the dominant cation on the exchange complex (Ca in CHL and Mg in SRP), in pH (5.4 vs 6.1 in CHL and SRP, respectively) and CHL was sandy-loam, while SRP was loamy. Additional details can be found in Falsone et al. (2007).

Extraction and characterization of mineral and organic phases

The mineralogical composition of the samples was evaluated through X-ray diffraction using a PW1810 diffractometer (40kV and 20 mA, Co Kα, graphite monochromator) on both the <2 mm sieved samples and

the clay fraction. The <2 mm samples were finely ground in an agate mortar and analyzed as air-dried randomly oriented powders from 3 to 80 º2θ at a speed of 0.6 º2θ min^{-1}. The clay fraction was separated by centrifugation after addition of sodium hexametaphosphate [$(NaPO_3)_6$] and analyzed as air-dried, ethylene glycol solvated, K-saturated, and heated (550°C) oriented mounts. Scans were made from 3 to 35 º2θ at a speed of 1 º2θ min^{-1}. A semiquantitative evaluation of mineral abundance was performed after background subtraction and calculation of peak intensities and positions using the second derivative option of the PowderX software (Dong, 1999).

The organic matter fraction was extracted from the organic horizons of both soils by treating the samples with 0.5M NaOH, followed by acidification to pH 1 with HCl and purification with a 0.1N HCl/0.3N HF solution (Swift, 1996). The purified fraction, i.e. the humic acid fraction, (HA) was then washed with deionized water until the solution pH was 3, freeze-dried and stored for further analysis. The two obtained HA fractions were labelled as HA-CHL and HA-SRP.

The elemental composition (C, N, H, S) of HAs was determined with an elemental analyzer (CE Instruments NA2100, Rodano, Italy); the O content was calculated by difference. The amount of total acidity and carboxyl groups was determined according to Schnitzer and Gupta (1965); the amount of phenolic –OH groups was calculated by difference. The absorbance ratio of HA solutions at 465 and 665 nm was used to determine the E_4/E_6 ratio (Chen et al., 1977). The absorbance was measured with an UV-Vis spectrophotometer (U-2000, Hitachi, Tokio, Japan).

The Fourier-Transform Infrared (FT-IR) spectra of HAs were recorded using pellets prepared by pressing 0.5 mg of humic substances with 200 mg of anhydrous KBr. Spectra were acquired from 4000 to 400 cm^{-1}, at 4 cm^{-1} resolution and 16 scans were averaged.

Incubation conditions

One hundred grams of the <2 mm air-dried samples of each soil were evenly distributed in a container and sprayed with a solution of HA containing 0.5 g of C_{HA}. To evaluate the effect of HA composition, each soil (CHL and SRP) was incubated with both HA fractions. Four aggregation tests were thus performed: CHL plus HA-CHL, CHL plus HA-SRP, SRP plus HA-CHL and SRP plus HA-SRP. The samples were allowed to dry for 2 weeks at room temperature. The experiment was replicated three times. At the end of the incubation period, the samples were sequentially dry sieved on 5- and 2-mm sieves, the aggregates remaining on each sieve (i.e. newly formed aggregates, NF) were weighed, and the result was expressed as percentage of the total mass (i.e., sum of <2, 2-5 and >5 mm fractions). The aggregation state was described by the Mean Weight Diameter (MWD) computed across *n* sieve size fractions using the relation:

$$MWD = \sum_{i=1}^{n} \bar{x}_i \, wi \qquad (1)$$

where $\bar{x}_i$ is the assumed diameter of the i^{th} fraction and w_i is the weight fraction retained on the i^{th} sieve-size. The aggregate diameter classes used in the MWD calculation were 0-2, 2-5 and 5-10 mm. The upper limit of the last aggregate diameter class was fixed on the basis of the observed greatest size of the NF-aggregates.

Characterization of newly formed aggregates

The analyses were done on the 2-5 mm NF-aggregates. The particle size distribution was determined by the pipette method (Gee & Bauder, 1986) after: (i) dispersion with $(NaPO_3)_6$; (ii) dispersion with deionized water only. The <2 µm fractions obtained were labelled as sodium-dispersible clay (NaDC) and water-dispersible clay (WDC). A first estimate of the colloidal stability was obtained by the clay dispersion ratio (CDR) calculated as the ratio between the mass (g kg^{-1}) of water-dispersible and sodium-dispersible clay (WDC/NaDC). On the WDC fraction, the electrophoretic mobility (EM) as a function of pH (from 2 to 6) was measured by laser Doppler velocimetry coupled with photon correlation spectroscopy using a DELSA 440 spectrometer (Beckman Coulter Electronics, Fullerton, CA) equipped with a 5-mW HeNe laser (632.8 nm). The point of zero charge was estimated by interpolating the two pH values for which the EM values were the closest to zero. The pH of the clay suspension was measured immediately before the electrochemical measurements. The Doppler shift arising from Brownian motion was used to determine the particle diffusion coefficient, which was converted to an equivalent hydrodynamic diameter using Stokes-Einstein equation as described by Hunter (1986). All measurements were run in duplicate.

The wet 2-5 mm NF-aggregate stability (WAS) was evaluated after 10 min in rotating 0.2-mm sieves. The material remaining on the sieves was then dried and weighed. The amount of stable aggregates (>0.2 mm) was corrected for the content of coarse sand determined after H_2O_2 oxidation. The WAS index was calculated as follows:

$$WAS = \frac{weight\ retained - weight\ of\ coarse\ sand}{total\ sample\ weight - weight\ of\ coarse\ sand} \cdot 100 \quad (2)$$

To test the wet cohesion independently from slaking, thus regardless of the ruptures due to water saturation, 10 g of NF aggregates were gently immersed into 95% solution of ethanol for 10 min (Le Bissonnais, 1996) before being wet sieved for 10 min. Then, the amount of aggregates that had resisted the sieving (WAS_{et}) was determined according to the equation (2).

The cumulative pore volume curve of NF-aggregates was determined using a Hg porosimeter (Porosimeter 2000 WS equipped with a Macropore unit 120, CE Instruments, Rodano, Italy). The total volume of intruded Hg (i.e. total pore volume) was expressed on a mass basis (V_{Hg}Tot, $mm^3\ g^{-1}$). The cumulative curve of intruded Hg volume as a function of the pore radius was used to calculate the variation of the pore volume as a function of the log-transformed radius, finding the slope between the pore radii Ri and Rj (Bruand & Prost, 1987):

$$slope_{ij} = \frac{V_i - V_j}{\log_{10} R_j - \log_{10} R_i} \quad (3)$$

where the volumes *Vi* and *Vj* correspond to the radii *Ri* and *Rj* at two successive positions *i* and *j*. The values of the slopes were plotted against the mean log radius. The relative maxima of the slope curve indicated the most represented classes of pores. Each peak thus corresponded to a radius that was termed modal radius (expressed in µm). The volume of each modal class of pores was thus included between two minimum values of the slope, which defined the limits of the class. This data treatment typically returns a bimodal distribution.

We thus labelled the modal pore radii as Rf and Rc and attributed them to the packing of finer (clay) and coarser (sand and silt), according to Fiès & Bruand (1998). The corresponding volumes of pores were labelled as $V_{Hg}f$ and $V_{Hg}c$. The packing density, i.e. the volume occupied by solid particles with respect to the total volume, was calculated according to Falsone & Bonifacio (2009) as:

$$packing\ density = \frac{particle\ mass}{particle\ density} \cdot \frac{1}{\frac{particle\ mass}{particle\ density} + volume\ of\ intruded\ Hg} \quad (4)$$

where particle density was taken equal to 2.65×10^{-3} g mm^{-3}, the mass was expressed in g (100 g)$^{-1}$, the volume of intruded Hg in mm^3 g^{-1}, and the resulting packing density was dimensionless. We calculated the packing density of clay using the NaDC fraction from textural analyses for particle mass and the modal volume corresponding to clay–clay interactions. The packing density of the sand and silt phases was also calculated, following the same assumptions.

Data analysis

To evaluate the relative importance of mineralogy and OM characteristics, the results of this study were matched to those obtained previously (Falsone et al., 2007) after one water-only wet-dry cycle. The parameters we considered were: % of 2-5 mm NF-aggregates, wet aggregate stability indexes, CDR, porosity data, and PZC and hydrodynamic diameter of WDC. The changes of each parameter were expressed as % variation calculated as:

$$\%\ variation = \frac{parameter\ value_{NF\ HA} - parameter\ value_{NF\ WD}}{parameter\ value_{NF\ WD}} \cdot 100$$

where *NF HA* and *NF WD* refer to the present and previous data, respectively. Differences in the % variation among samples were evaluated by means of the analysis of variance (ANOVA and Duncan's test). Before analysis, the homogeneity of variances was checked using the Levene test and the normality of data through the Shapiro-Wilks test. The threshold used for significance in all statistical tests was set at 0.05. All data treatments were carried out using SPSS 20 (SPSS Inc., Chicago, IL).

RESULTS

Mineralogical and soil organic matter characteristics

The two samples showed similar mineralogical species but sharply differ in their proportions (Figure 1). In the <2 mm fraction, serpentines were the most abundant minerals in SRP (>30%), followed by chlorite, quartz, Na-feldspars (albite), amphiboles, lithogenic micas (phlogopite), K-feldspars (orthoclase) and illite. In the CHL sample instead the most abundant mineral was chlorite (~20%), but large amounts of feldspars (around 15%, both orthoclase and albite) were present, as well as lithogenic micas (margarite), talc and amphiboles (~10%). Small amounts of serpentines and quartz were found as well. More differences between the two samples were visible in the clay fraction: in SRP serpentine dominated (~60%), associated with minor amounts of chlorite and swelling mixed-layer minerals, with traces of amphiboles, illite and illitic mixed-layers. In CHL

chlorite was the most abundant mineral (~50%), followed by talc, serpentine, illite, chlorite-illite randomly interstratified minerals and traces of amphiboles.

The carbon content of oxidized organic matter fractions from the CHL organic horizon was significantly lower ($p<0.05$, $n=6$) than that of SRP (Table 1), while the opposite was observed for the N content. The C/N molar ratio was consequently minor in CHL, indicating a higher degree of decomposition and/or a larger incorporation of N containing organic compounds. The H/C and O/C molar ratios, significantly higher in CHL than in SRP ($p<0.05$, $n=6$), suggested a larger contribution of the cellulosic component in the former. Higher H/C ratios indicate indeed that the organic matter fraction from CHL is more aliphatic than SRP, while the O/C ratio specifies the presence of O–containing functional groups, such as the –OH groups in the cellulose polymers and carboxyl (–COOH) groups deriving from oxidation processes. This was confirmed by chemical titration and FT-IR spectra (Figure 2). The HA from CHL had more carboxyl groups than SRP, but less phenolic –OH groups ($p<0.05$, $n=6$, Table 1). The higher acidity found in SRP was coupled to a higher E_4/E_6 ratio, indicating a lower molecular size and a higher charge/mass ratio with respect to CHL. This ratio gives indeed an estimate of the molecular size and presence of charged functional groups: the higher the E_4/E_6 ratio, the smaller the size and the higher the charge (Chen et al., 1977). Although the FT-IR spectra of HAs appeared similar (Figure 2), they showed some specific differences, such as the peaks at about 1631 and 1514 cm^{-1} (aromatic C=C stretching), more pronounced in SRP, a band at 1534 cm^{-1} (-CONH- stretching of II amides) visible only in CHL, and a band in the region 1060-1034 cm^{-1} (polysaccharide C–O stretching) more pronounced in CHL. The HA from CHL appeared therefore to be richer in cellulosic and proteinaceous residues, more oxidized, with a higher content of carboxyl groups, whereas HA-SRP was more aromatic and richer in phenolic groups.

Properties of the NF- macroaggregates

From 100 g of the CHL fine earth we obtained on the average 18.8 and 9.8 g of 2-5 and >5 mm NF aggregates, whereas the yield was 29.7 and 15.3 g for SRP, respectively (Table 2). The MWD value was consequently significantly higher ($p<0.05$, $n=6$) in SRP samples than in CHL. No relevant differences between the two HAs were found.

After 10 min of wet sieving, the 2-5 mm NF aggregates of CHL were more fragile than those of SRP, with WAS values of 63.0 and 71.8% on average, respectively (Table 3). However, when the initial slaking was avoided, the samples had similar WAS_{et} values (72.8 and 74.6% on average) showing a comparable resistance against water abrasion. The total volume of Hg intruded in the pores of 2-5 mm NF aggregates ($V_{Hg}Tot$) ranged from 177 to 188 $mm^3\ g^{-1}$. The analysis of the cumulative curve of the intruded Hg volume allowed to identify a bimodal distribution of pores in all samples (data not shown) attributed to the coarser particles, i.e. silt and sand, and to the finer colloidal phase according to Fiès & Braund (1998). The modal pore of coarser particles (Rc) was more than three times higher in CHL than in SRP ($p<0.05$, $n=12$). The packing density of coarser particles, i.e. silt and sand, was similar, with no effect of the origin of HAs, and corresponded to orthorhombic-rhombohedral particle arrangement (Lal & Shukla, 2004).

256

257 *Properties of the colloidal phases*

258 The colloidal behaviour greatly differed between samples. The CDR values were <0.4 in CHL and >0.8 in
259 SRP ($p<0.05$, n=12, Table 3), thus less than 40% clay was water dispersible (WDC) in CHL and more than
260 80% in SRP. The electrophoretic mobility of WDC varied as a function of pH from +0.25 to -0.65 µm cm s^{-1}
261 V^{-1} in CHL; in SRP from +0.27 to -0.52 µm cm s^{-1} V^{-1} (Figure 3). No effect of the origin of HAs was visible
262 in CHL, while in SRP the addition of HA-SRP induced a lower electrophoretic mobility at the lowest pH than
263 HA-CHL ($p<0.05$, n=6). The point of zero charge (PZC) of both samples was however around pH 2-2.5, and
264 only slightly lower (<2) in the case of SRP with HA-SRP. At the lowest pH, the hydrodynamic diameter of
265 CHL particles was on average slightly smaller than that of SRP (Table 3), and with increasing pH, changes in
266 the electrophoretic mobility were accompanied by a decrease in particle size.
267 The size of Rf, i.e. the modal radius of voids originated by the arrangement of clay particles, was always lower
268 than 0.02 µm and its variability was small among samples (data not shown). The volume of the modal fine
269 pores ($V_{Hg}f$) was small, and CHL had lower values than SRP (Table 3). The packing density of the clay phase
270 was instead significantly higher in CHL ($p<0.05$, n=12), and solids may occupy as much as 87-94% of the
271 total volume, corresponding to a very close rhombohedral arrangement of clays.
272

273 *HA addition effect*

274 In order to compare the results obtained in the four treatments (i.e. two soils and two HAs), hence to understand
275 both the effect of HA addition and differing mineralogical composition, the data were matched to those
276 obtained in a previous experiment in which the wet-dry cycle was performed with deionized water only
277 (Falsone et al., 2007).
278 The mass of the 2-5 mm NF aggregates generally increased after the addition of HA with respect to the water-
279 only wet-dry cycle (Figure 4A). SRP showed the smallest positive variation, but no significant differences
280 among samples were visible. Aggregate stability (both WAS and WAS_{et} indexes) was negatively or poorly
281 affected by HA addition in SRP (Figure 4B, C). This was coupled with a decrease in the volume of coarser
282 pores and an increase in packing density of coarser fraction (Figure 4D, E). Instead CHL HA-added samples
283 were more stable to water abrasion (i.e. WAS_{et} increased), and no variations in $V_{Hg}C$ and PDc were found. The
284 results obtained in CHL were thus generally significantly different ($p<0.05$, n=12) from those in SRP (Figure
285 4). The differences at macroaggregate scale hence appeared more related to the soil mineralogical composition.
286 A significantly different response between samples ($p<0.05$, n=12) was also found for the colloidal phase. In
287 fact, with respect to the water-only wet-dry cycle, the dispersibility and size at the lowest pH of the clay fraction
288 of HA-added SRP samples increased (Figure 5A, E) and the PZC decreased (Figure 5D). The $V_{Hg}f$ increased
289 in SRP (Figure 5B) and the clay particles had a more open arrangement than in the case of the wet-dry cycle
290 incubation (Figure 5C). In CHL an opposite trend was generally observed, with the exception of PZC values.
291 In fact, upon HA addition, the PZC was reached at lower pH also in CHL although the differences were smaller
292 than in SRP. No significant differences related to the HA origin were observed, with the exception of the

293 hydrodynamic diameter (Figure 5).
294
295
296 **DISCUSSION**
297 Differences in sample response upon addition of organic matter, at both macroaggregate and colloidal size
298 scale, were found to be largely dependent on mineralogical composition. The serpentinitic soil (SRP) had a
299 higher macroaggregate formation capacity, and aggregates were more stable than in the chloritic one (CHL),
300 especially against slaking losses. Moreover, the colloidal phase was less dispersible and WDC had a higher
301 electrophoretic mobility in CHL than SRP, although both had a relatively low negative charge with respect to
302 the most common Al-phyllosilicates (Celi et al., 1999). All these findings reflect the aggregation pathways
303 observed in the previous experiment on the effect of wet-dry cycles that can be summarized as dominated by
304 clay-clay interactions in CHL and clay-sand interactions in SRP (Falsone et al., 2007).
305 With respect to the water-only wet-dry cycle, the addition of oxidized organic matter enhanced aggregate
306 formation in both samples but improved aggregate stability towards abrasion only in CHL. In addition, the
307 clay fraction of HA-added CHL samples was less dispersible, although only slight differences in charge
308 properties of the dispersed particles were visible. The $V_{Hg}f$ decreased in CHL and the clay particles had a
309 denser arrangement than in the case of the previous experiment. In HA added SRP an opposite trend was
310 observed, and generally the differences were more pronounced, with a PZC at lower pH and larger
311 hydrodynamic diameter than the water-only wet-dry treated SRP samples. The addition of humic substances
312 on soil (Plaza et al., 2014), oxides (Li et al., 2015) and clay minerals (Majzik & Tombácz, 2007) has a strong
313 effect on surface charge and particle dispersibility, mostly because of the polyelectrolyte nature of HA that
314 increases the net negative charge. The higher flocculation in CHL may be related to a larger abundance of
315 reactive clay surfaces (Vogel et al., 2014), also favoured by the greater presence of Ca on the exchange
316 complex, which can thus form more stable bonds with the organic material (Bronick & Lal, 2005). In CHL,
317 clay particles and HA could thus form a more compact arrangement through clay-Ca-HA, as shown by the PDf
318 increase. The possibility of direct bonding between negatively charged clay surfaces and positive amino groups
319 of proteinaceous remains, abundant in HA-CHL, as well as the interaction of $–COO^-$ groups with mineral edge
320 Me–OH by ligand exchange, cannot be ruled out from electrophoretic mobility data, but cation bridges seem
321 to dominate as no differences between the two HAs were found. Calcium bridges may therefore add to clay-
322 clay interactions in aggregate formation and contribute to the greater stability against abrasion in CHL. The
323 added organic material contribute therefore in this soil to the aggregation process while, being retained into
324 aggregates, had little or no effect on the water dispersible fraction.
325 The larger abundance of Mg, more hydrated than Ca, in the SRP soil might have favoured instead weaker
326 outer-sphere interactions with HA. The presence of HA on clay surfaces has probably hindered the formation
327 of clay coatings on sand grains (Falsone et al. 2007), decreasing aggregate stability and allowing the dispersion
328 of more negatively charged mineral-HA associated particles with respect to the water-only wet-dry conditions.
329 The chemical composition of HA influenced therefore the charge characteristics of WDC: the higher contents

of amino groups in HA-CHL than in HA-SRP induced a higher positive charge at low pH, while the higher carboxyl content made the surfaces more negative at pH higher than the point of zero charge. Phenolic groups may contribute to the negative charge only at pH > 6.0 (Alvarez-Puebla & Garrido, 2005) justifying the less negative electrophoretic mobility obtained with HA-SRP at pH 4.0. As upon HA addition the surface of WDC still carried a positive charge at low pH, stable bonds such as ligand exchange may be ruled out. In addition, since low amounts of HA are sufficient to reverse the mineral charge even at low pH, the amount of HA on clay surfaces was probably very low (Magnacca et al., 2014).

CONCLUSIONS

Organic matter inputs on the fine earth fraction of a serpentinitic and a chloritic soil promoted the formation of new aggregates in the size range of 2-5 and >5 mm, even if their wet stability was not always positively affected. The soil response however mostly depended on mineralogical composition, with no effect of HA composition on aggregates but only on the surface charge of the dispersible clay particles.

In soils dominated by Mg-silicates, weak chemical interactions between organic matter and mineral particles are the most important mechanism in controlling both aggregation processes and clay dispersibility. Ligand exchange reactions, if any, seem to be of only minor importance, stressing the differences with Al-silicates.

Because of the complex interlink between mineralogy, organic matter characteristics and dominant cations, the addition of organic matter may even favour the dispersion of OM-loaded clay particles, confounding the expected positive effects against land degradation.

ACKNOWLEDGEMENTS

This research was funded by Università di Torino, Fondo Ricerca Locale (ex 60%)

REFERENCES

Abiven S, Menasseri S, Chenu C. 2009. The effects of organic inputs over time on soil aggregate stability – A literature analysis. Soil Biology and Biochemistry 41: 1-12. DOI: 10.1016/j.soilbio.2008.09.015

Adhikari K, Hartemink AE. 2016. Linking soils to ecosystem services – A global review. Geoderma 262: 101-111. DOI: 10.1016/j.geoderma.2015.08.009

Alvarez-Puebla RA, Garrido JJ. 2005. Effect of pH on the aggregation of a gray humic acid in colloidal and solid state. Chemosphere 59: 659-667. DOI: 10.1016/j.chemosphere.2004.10.021

Andruschkewitsch R, Geisseler D, Dultz S, Joergensen RG, LudwigB.2014. Rate of soil-aggregate formation under different organic matter amendments - a short-term incubation experiment. Journal of Plant Nutrition and Soil Science 177: 297-306. DOI: 10.1002/jpln.201200628297

Arjmand Sajjadi S., Mahmoodabadi M. 2015. Aggregate breakdown and surface seal development influenced by rain intensity, slope gradient and soil particle size. Solid Earth 6: 311-321. DOI: 10.5194/se-6-311-2015

Berendse F, van Ruijven J, Jongejans E, Keesstra S. 2015. Loss pf plant species diversity reduces soil erosion resistance. Ecosystems 18: 881-888. DOI: 10.1007/s10021-015-9869-6

Brevik EC, Cerdà A, Mataix-Solera J, Pereg L, Quinton JN, Six J, Van Oost K. 2015. The interdisciplinary nature of *SOIL*. SOIL 1: 117-129. DOI:10.5194/soil-1-117-2015

Bronick CJ, Lal R. 2005. Soil structure and management: a review. Geoderma 124: 3-22. DOI: 10.1016/j.geoderma.2004.03.005

Bruand A, Prost R. 1987. Effect of water content on the fabric of soil material: an experimental approach. European Journal of Soil Science 38: 461–472. DOI: 10.1111/j.1365-2389.1987.tb02281.x

Celi L, Lamacchia S, Ajmone Marsan F, Barberis E. 1999. Interaction of inositol hexaphosphate on clays: Adsorption and charging phenomena. Soil Science 164: 574-585.

Cerdà, A. 1996. Soil aggregate stability in three Mediterranean environments. Soil Technology 9: 133-140. DOI: 10.1016/S0933-3630(96)00008-6

Cerdà A. 2000. Aggregate stability against water forces under different climates on agriculture land and scrubland in southern Bolivia. Soil and Tillage Research 36: 1- 8. DOI: 10.1016/S0167-1987(00)00155-0

Chaplot V, Cooper M. 2015. Soil aggregate stability to predict organic carbon outputs from soils. Geoderma 243-244: 205-213. DOI: 10.1016/j.geoderma.2014.12.013

Chen Y, Senesi N, Schnitzer M. 1977. Information provided on humic substances by E4/E6 ratios. Soil Science Society of America Journal 41: 353-358. DOI:10.2136/sssaj1977.03615995004100020037x

Denef K, Six J, Merckx R, Paustian K. 2002. Short-term effects of biological and physical forces on aggregate formation in soils with different clay mineralogy. Plant and Soil 246: 185-200. DOI: 10.1023/A:1020668013524

Debasish-Saha, Kukal SS, Bawa SS. 2014. Soil organic carbon stock and fractions in relation to land use and soil depth in the degraded Shiwaliks hills of lower Himalayas. Land Degradation and Development 25: 407–416. DOI: 10.1002/ldr.2151

De Clercq T, Heiling M, Dercon G, Resch C, Aigner M, Mayer L, Mao Y, Elsen A, Steier P, Leifeld J, Merckx R. 2015. Predicting soil organic matter stability in agricultural fields through carbon and nitrogen stable isotopes. Soil Biology and Biochemistry 88: 29-38. DOI: 0.1016/j.soilbio.2015.05.011

de Oliveira SP, de Lacerda N B, Blum SC, Escobar MEO, de Oliveira TS. 2015., Organic Carbon and Nitrogen Stocks in Soils of Northeastern Brazil Converted to Irrigated Agriculture, Land Degradation and Development 26: 9–21. DOI: 10.1002/ldr.2264

Ding GC, Geertje JP, Babin D, Heuer H, Heister K, Kögel-Knabner I, Smalla K. 2013. Mineral composition and charcoal determine the bacterial community structure in artificial soils. FEMS Microbiology Ecology 86: 15-25. DOI:10.1111/1574-6941.12070

Dong C. 1999. PowderX: Windows-95 based program for powder X-ray diffraction data processing. Journal of Applied Cristallography 32: 838–838. DOI: 10.1107/S0021889899003039

Codice campo modificato

403 Falsone G, Bonifacio E. 2009. Pore-size distribution and particle arrangement in fragipan and nonfragipan
404 horizons. Journal of Plant Nutrition and Soil Science 172:696-703. DOI: 10.1002/jpln.200800066
405 Falsone G, Celi L, Bonifacio E. 2007 Aggregate formation in chloritic and serpentinitic alpine soils. Soil
406 Science 172: 1019-1030. DOI: 10.1097/ss.0b013e31815778a0
407 Fiès JC, Bruand A. 1998: Particle packing and organization of the textural porosity in clay-silt-sand
408 mixtures. European Journal of Soil Science 49: 557–567. DOI: 10.1046/j.1365-2389.1998.4940557.x
409 Gee GW, Bauder JW. 1986. Particle-size analysis. In: Methods of Soil Analysis, Part 1.Physical and
410 Mineralogical Methods. A Klute (ed.). Agron. Monogr. n. 9. ASA and SSSA, Madison, WI, pp. 383–
411 411
412 Gelaw A M, Singh B R, Lal R. 2015. Organic carbon and nitrogen associated with soil aggregates and
413 particle sizes under different land uses in Tigray, northern Ethiopia. Land Degradation and
414 Development 26: 690-700. DOI: 10. 1002/ldr
415 Gümüs I, Şeker C. 2015. Influence of humic acid applications on modulus of rupture, aggregate stability,
416 electrical conductivity, carbon and nitrogen content of a crusting problem soil. Solid Earth 6: 1231-
417 1236. DOI: 10. 5194/se-6-1231-2015
418 Hunter R J. 1986. Foundations of Colloid Science. Vol I. Oxford University Press, New York.
419 Keesstra SD, Geissen V, Mosse K, Piiranen S, Scudiero E, Leistra M, van Schaik L. 2012. Soil as a filter for
420 groundwater quality. Current Opinion in Environmental Sustainability 4: 507-5016. DOI:
421 10.1016/j.cosust.2012.10.007
422 Kögel-Knabner I, Guggenberger G, Kleber M, Kandeler E, Kalbitz K, Scheu S, Eusterhues K, Leinweber P.
423 2008. Organo-mineral associations in temperate soils: Integrating biology, mineralogy, and organic
424 matter chemistry. Journal of Plant Nutrition and Soil Science 171: 61-82.
425 DOI:10.1002/jpln.200700048
426 Lal R, Shukla MK. 2004. Soil Structure. In: Principles of Soil Physics. R Lal and MK Shukla (eds). Marcel
427 Dekker, New York, pp. 93–148
428 Le Bissonnais Y. 1996. Aggregate stability and assessment of soil crustability and erodibility: I. Theory and
429 methodology. European Journal of Soil Science 47: 425–437. DOI: 10.1111/j.1365-
430 2389.1996.tb01843.x
431 Legros JP. 1992. Soils of Alpine mountains. In: Weathering soils and paleosoils. Martini and Chesworth
432 (eds). Developments in Earth Surface Processes, n. 2. Elsevier, Amsterdam, 155-181.
433 Li Y, Yang C, Guo X, Dang Z, Li X, Zhang Q. 2015. Effects of humic acids on the aggregation and sorption
434 of nano-TiO_2. Chemosphere 119: 171-176. DOI: 10.1016/j.chemosphere.2014.05.002
435 Majzik A, Tombácz E. 2007. Interaction between humic acid and montmorillonite in the presence of calcium
436 ions I. Interfacial and aqueous phase equilibria: adsorption and complexation. Organic Geochemistry
437 38: 1319-1329. DOI: 10.1016/j.orggeochem.2007.04.003
438 Magnacca G, Allera A, Montoneri E, Celi L, Benito DE, Gagliardi LG, Gonzalez MC, Mártire DO, Carlos L.
439 Novel magnetite nanoparticles coated with waste-sourced biobased substances as sustainable and

440 renewable adsorbing materials. ACS Sustainable Chemistry and Engineering 2: 1518-1524. DOI:
441 10.1021/sc500213j
442 Mamedov AI, Bar-Yosef B, Levkovich I, Rosenberg R, Silber A, Fine P, Levy GJ. 2014. Amending soil with
443 sludge, manure, humic acid, orthophosphate and phytic acid: Effects on aggregate stability. Soil
444 Research 52: 317-326. DOI: 10.1071/SR13334
445 Mataix-Solera J, Cerdà A, Arcenegui V, Jordán A, Zavala LM. 2011. Fire effects on soil aggregation: A
446 review. Earth-Science Reviews 109: 44-60. DOI: 10.1016/j.earscirev.2011.08.002
447 Mikutta R, Mikutta C, Kalbitz K, Scheel T, Kaiser K, Jahn R. 2007. Biodegradation of forest floor organic
448 matter bound to minerals via different binding mechanisms. Geochimica et Cosmichimica Acta 71:
449 2569-2590. DOI: 10.1016/j.gca.2007.03.002
450 Mizuta K, Taguchi S, Sato S. 2015. Soil aggregate formation and stability induced by starch and cellulose.
451 Soil Biology and Biochemistry 87: 90-96. DOI: 10.1016/j.soilbio.2015.04.011
452 Muñoz-Rojas M, Jordán A, Zavala LM, De la Rosa D, Abd-Elmabod SK, Anaya-Romero M. 2015. Impact
453 of Land Use and Land Cover Changes on Organic Carbon Stocks in Mediterranean Soils (1956–2007).
454 Land Degradation and Development 25: 168–179. DOI: 10.1002/ldr.2194
455 O'Rourke SM, Angers DA, Holden NM, McBratney AB. 2015. Soil organic carbon across scales. Global
456 Change Biology. DOI: 10.1111/gcb.12959,
457 Piccolo A, Mbagwu JSC. 1999. Role of hydrophobic components of soil organic matter on the stability of
458 soil aggregates. Soil Science Society of America Journal 63: 1801–1810.
459 DOI:10.2136/sssaj1999.6361801x
460 Plaza I, Ontiveros-Ortega A, Calero J, Aranda V. 2014. Implication of zeta potential and surface free energy
461 in the description of agricultural soil quality: effect of different cations and humic acids on degraded
462 soils. Soil and Tillage Research 146: 148-158. DOI: 10.1016/j.still.2014.10.013
463 Regelink IC, Stoof CR, Rousseva S, Weng L, Lair GJ, Kram P, Nikolaidis NP, Kercheva M, Banwart S,
464 Comans RNJ 2015. Linkages between aggregate formation, porosity and soil chemical properties.
465 Geoderma 247-248: 24-37. DOI: 10.1016/j.geoderma.2015.01.022
466 Schnitzer ME, Gupta VC. 1965. Determination of acidity in soil organic matter. Soil Science Society of
467 America Proceedings 29: 274-277
468 Seeger M, Ries JB. 2008. Soil degradation and soil surface process intensities on abandoned fields in
469 Mediterranean mountain environments. Land Degradation and Development 19: 488–501, DOI:
470 10.1002/ldr.854
471 Six J, Paustian K. 2014. Aggregate-associated soil organic matter as an ecosystem property and a
472 measurement tool. Soil Biology and Biochemistry 68: A4-A9. DOI: 10.1016/j.soilbio.2013.06.014
473 Six J, Bossuyt H, Degryze S, Denef K. 2004. A history of research on the link between (micro)aggregates,
474 soil biota, and soil organic matter dynamics. Soil and Tillage Research 79: 7-31. DOI:
475 10.1016/j.still.2004.03.008

476 Stanchi S, Falsone G, Bonifacio E. 2015. Soil aggregation, erodibility, and erosion rates in mountain soils
477 (NW Alps, Italy). Solid Earth 6: 403–414. DOI: 10.5194/se-6-403-2015
478 Soil Survey Staff. 2014. Keys to Soil Taxonomy, 12th ed. USDA-Natural Resources Conservation Service,
479 Washington, DC.
480 Swift RS. 1996. Organic matter characterization. In: Methods of Soil Analysis: Chemical Methods, 3rd Ed.
481 D. L Sparks (ed.). ASA and SSSA, Madison, WI, pp. 1011–1070
482 Vogel C, Babin D, Pronk GJ, Heister K, SmallaK, Kögel-Knabner I. 2014. Establishment of macro-
483 aggregates and organic matter turnover by microbial communities in long-term incubated artificial
484 soils. SoilBiology and Biochemistry 79: 57-67. DOI:10.1016/j.soilbio.2014.07.012
485 Vogel C, Mueller CW, Höschen C, Buegger F, Heister K., Schulz S, Schloter M, Kögel-Knabner I. 2014.
486 Submicron structures provide preferential spots for carbon and nitrogen sequestration in soils. Nature
487 Communications 5: 2947. DOI:10.1038/ncomms3947
488 Zhang K, Zheng H, Chen FL, Ouyang ZY, Wang Y, Wu YF, Lan J, Fu M, Xiang XW. 2015. Changes in soil
489 quality after converting Pinus to Eucalyptus plantations in southern China. Solid Earth 6: 115-123.
490 doi:10.5194/se-6-115-2015
491 Zornoza R, Acosta JA, Bastida F, Domínguez SG, Toledo DM, Faz A. 2015. Identification of sensitive
492 indicators to assess the interrelationship between soil quality, management practices and human
493 health. SOIL 1: 173-185. DOI:10.5194/soil-1-173-2015
494

Table 1. Mean (± standard deviation) of elemental content, total acidity, carboxyl groups, and E_4/E_6 ratio of purified, ash and moisture-free HAs extracted from the CHL and SRP organic horizons (HA-CHL and HA-SRP, respectively). The letters show the significant differences at p level <0.05 (Duncan's test) between HA (n=6)

	HA-CHL	HA-SRP
ash (%)	1.6±0.3	1.2±0.1
C (%)	50.51±0.31^b	54.59±0.61^a
N (%)	5.51±0.27^a	3.59±0.26^b
H (%)	6.13±0.04	6.16±0.09
S (%)	0.64±0.01^a	0.30±0.03^b
O (%)	37.21±0.33	35.35±0.80
C/N	10.69±0.54^b	17.72±1.07^a
H/C	1.45±0.01^a	1.35±0.04^b
O/C	0.55±0.01^a	0.49±0.02^b
total acidity (cmol kg^{-1})	566±8^b	608±11^a
-COOH (cmol kg^{-1})	254±6^a	232±3^b
Phenolic OH (cmol kg^{-1})	312±1^b	376±8^a
E_4/E_6	6.20±0.08^b	6.57±0.08^a

-COOH: carboxyl groups; Phenolic OH: phenolic OH-groups; E_4/E_6: ratio of absorbance at 465 and 665 nm

502 Table 2. Mean (± standard deviation) of percentage of newly-formed aggregate classes and aggregate Mean
503 Weight Diameter (MWD). The letters show the significant differences at *p* level <0.05 (Duncan's test)
504 between treatments within each site (n=6; lowercase letters) and between sites (n=12; uppercase letters)

505

soil sample	treatment	2-5 mm (%)	>5 mm (%)	MWD (mm)
CHL	HA-CHL	19.6±1.6	9.1±0.7	2.08±0.01
	HA-SRP	17.5±3.6	10.3±2.5	2.10±0.23
	mean±st. dev	18.8±2.9 ^{B}	9.8±1.9^{B}	2.10±0.16^{B}
SRP	HA-CHL	33.2±3.4^{a}	14.4±1.6	2.77±0.19
	HA-SRP	27.4±2.5^{b}	15.9±4.6	2.72±0.28
	mean±st. dev	29.7±4.0^{A}	15.3±3.4^{A}	2.74±0.22^{A}

506

Table 3. Mean (± standard deviation) of stability indexes of 2-5 mm newly-formed aggregates (WAS and WAS_{et}) and of the colloidal phase (CDR), porosity data of coarser particles (i.e. sand and silt), and characteristics of the colloidal phases obtained from newly-formed aggregates. The letters show the significant differences at p level <0.05 (Duncan's test) between treatments within each site (n=6; lowercase letters) and between sites (n=12; uppercase letters)

soil sample	CHL			SRP		
treatment	HA-CHL	HA-SRP	*mean±dev.st*	HA-CHL	HA-SRP	*mean±dev.st*
WAS (%)	61.0±1.4^{b}	64.9±1.1^{a}	63.0±2.5^{B}	71.6±0.7	72.0±1.3	71.8±0.9^{A}
WAS_{et} (%)	73.8±1.8^{a}	71.8±1.8^{b}	72.8±1.9	77.0±1.7^{a}	72.2±2.5^{b}	74.6±3.3
V_{Hg}Tot (mm^3 g^{-1})	180±11	177±9	178±10	177±25	188±23	183±43
V_{Hg}c (mm^3 g^{-1})	178±9	176±9	177±10	173±22	175±18	174±43
Rc (µm)	1.494±0.272	1.809±0.279	1.651±0.349^{A}	0.450±0.129	0.470±0.012	0.460±0.076^{B}
PDc	0.67±0.01	0.67±0.01	0.67±0.01	0.68±0.03	0.68±0.02	0.68±0.05
CDR	0.38±0.04	0.30±0.03	0.34±0.06^{B}	0.86±0.05	0.94±0.04	0.90±0.07^{A}
hydrodynamic diameter at the lowest pH (µm)	1.05±0.14^{a}	0.83±0.04^{b}	0.94±0.15	0.92±0.10	1.08±0.17	1.00±0.17
hydrodynamic diameter at the highest pH (µm)	0.72±0.10	0.78±0.07	0.75±0.08	0.71±0.03	0.71±0.02	0.71±0.02
V_{Hg}f (mm^3 g^{-1})	2±1	1±<1	1±1	5±4	14±5	9±6
PDf	0.87±0.08	0.94±0.04	0.91±0.06^{A}	0.73±0.17	0.52±0.09	0.62±0.16^{B}

WAS: wet aggregate stability; WAS_{et}: wet aggregate stability after ethanol saturation; V_{Hg}Tot: total volume of intruded Hg (i.e. total pore volume); V_{Hg}c: volume of pores within the coarser particles; Rc: modal radius of packing of coarser particles; PDc: packing density of the coarser particles; CDR: clay dispersion ratio; V_{Hg}f: volume of pores within the finer particles; PDf: packing density of the finer particles

Captions to Figures

Figure 1 – Mineral composition of bulk (<2 mm) and clay fractions of the CHL and SRP soil samples

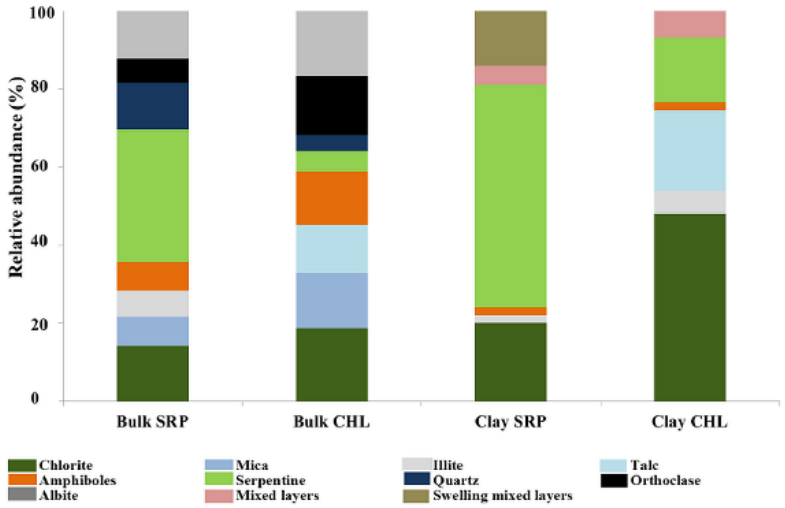

Figure 2 - FT-IR spectra of humic acids from the topsoil of CHL and SRP

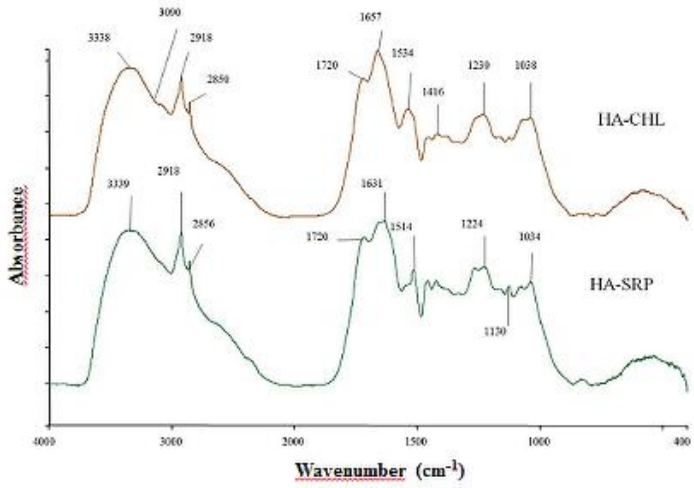

Figure 3 - Electrophoretic mobility (EM) values of WDC fraction of 2-5 NF aggregates obtained after HA addition in CHL (A) and SRP (B). Bars represent standard deviation

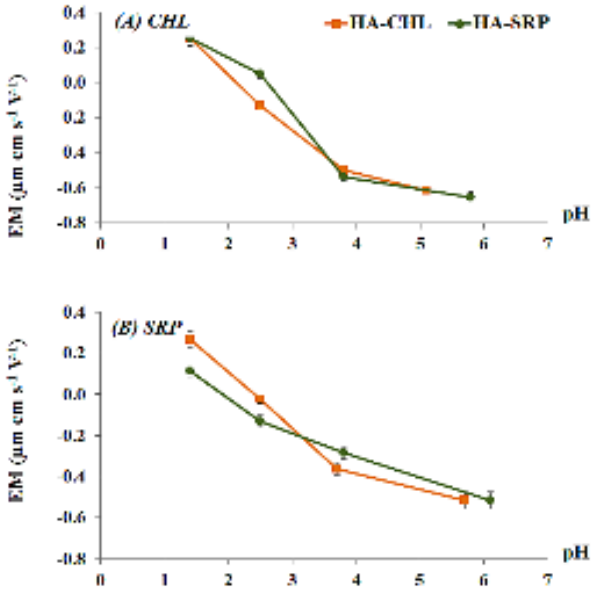

Figure 4 – Variations in the characteristics of 2-5 NF aggregates after HA addition with respect to water-only wet-dry experiment. Percentage changes in mass of aggregates (A), WAS (B), WAS_{et} (C) and porosity data of coarser particles of NF-macroaggregates (D, E). Bars represent standard deviation (SD). For graphical reasons SDs <1% were not reported. The letters show the significant differences at p level <0.05 (Duncan's test) among the four treatments

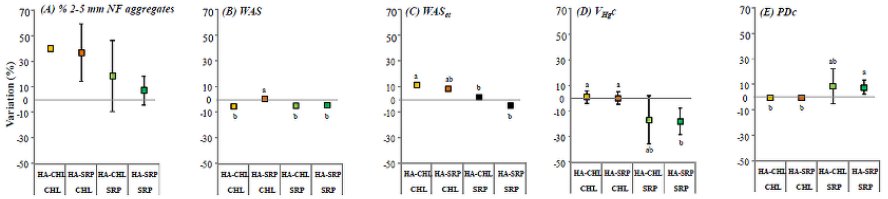

Figure 5 – Variations in the characteristics of water dispersible clay from NF aggregates after HA addition with respect to water-only wet-dry experiment. Percentage changes in CDR (A), porosity data of finer particles (B, C), PZC (D) and equivalent hydrodynamic diameter (E). Bars represent standard deviation (SD). For graphical reasons SDs <5% were not reported. The letters show the significant differences at p level <0.05 (Duncan's test) among the four treatments